Fluidic patch antenna based on liquid metal alloy/single-wall carbon-nanotubes operating at the S-band frequency

Cite as: Appl. Phys. Lett. **103**, 063101 (2013); https://doi.org/10.1063/1.4817861
Submitted: 26 April 2013 • Accepted: 24 July 2013 • Published Online: 06 August 2013

B. Aïssa, M. Nedil, M. A. Habib, et al.

Fluidic patch antenna based on liquid metal alloy/single-wall carbon-nanotubes operating at the S-band frequency

B. Aïssa,[1,2,3,a)] M. Nedil,[4] M. A. Habib,[5] E. Haddad,[1] W. Jamroz,[1] D. Therriault,[2] Y. Coulibaly,[4] and F. Rosei[3]

[1]*Department of Smart Materials and Sensors for Space Missions, MPB Technologies, Inc., 151 Hymus Boulevard, Montreal H9R 1E9, Canada*
[2]*Center for Applied Research on Polymers (CREPEC), Mechanical Engineering Department, École Polytechnique de Montréal, P.O. Box 6079, Montreal H3C 3A7, Canada*
[3]*Centre Énergie, Matériaux et Télécommunications, INRS, 1650, Boulevard Lionel-Boulet Varennes, Quebec J3X 1S2, Canada*
[4]*Laboratoire de Recherche Télébec en Communications Souterraines, UQAT. 450, 3e Avenue, Val-d'Or J9P 1S2, Canada*
[5]*Department of Computer Science, Yanbu University College, P.O. Box 30031, Kingdom of Saudi Arabia*

(Received 26 April 2013; accepted 24 July 2013; published online 6 August 2013)

This letter describes the fabrication and characterization of a fluidic patch antenna operating at the S-band frequency (4 GHz). The antenna prototype is composed of a nanocomposite material made by a liquid metal alloy (eutectic gallium indium) blended with single-wall carbon-nanotube (SWNTs). The nanocomposite is then enclosed in a polymeric substrate by employing the UV-assisted direct-writing technology. The fluidic antennas specimens feature excellent performances, in perfect agreement with simulations, showing an increase in the electrical conductivity and reflection coefficient with respect to the SWNTs concentration. The effect of the SWNTs on the long-term stability of antenna's mechanical properties is also demonstrated. © *2013 AIP Publishing LLC*. [http://dx.doi.org/10.1063/1.4817861]

The past decade has witnessed the rapid growth of communication and sensing applications, leading to an escalating demand for advances in antenna technologies,[1–3] including mobile communications,[4] compact high gain patch antenna,[5] or the multiple-input multiple-output (MIMO) channel technologies.[6] Although copper and other solid conductors can provide highly efficient antennas, the fatigue of copper even in the form of thin foil does not allow antennas to be continually deformed for general adaptive antenna applications. Flexible antennas have the potential to enhance the emerging field of flexible electronics.[7,8] Bendable antennas are also of interest for "smart antenna" applications such as beam-forming and beam-bending,[9] antennas for limited and nonplanar spaces,[10] and antennas for wearable health-monitoring devices, aeronautic remote sensing, or wireless strain sensors using printed radio frequency identification (RFID) tags.[3,11–13]

Flexible antennas fabricated based on polydimethylsiloxane (PDMS) and liquid metal alloys have recently been demonstrated.[14–24] For instance, Cheng *et al.*[15] and So and coworkers[14] reported an unbalanced loop antenna and a half-wave dipole antenna that were fabricated by injecting gallium indium tin (Galinstan, Ga 68.5%, In 21.5%, and Sn 10%) and eutectic gallium indium alloy (EGaIn, Ga 75.5%, and In 24.5%) into microfluidic channels in elastic PDMS substrates.

On the other hand, Kim *et al.*[25,26] recently described stretchable integrated circuits with elongation of up to 100% using wavy, thin silicon ribbons on elastic substrates. Besides its ability to produce flexible antennas, this fluidic-method has additional advantages: (i) The process is fairly simple and scalable and can be adopted to other flexible 2D and 3D devices; (ii) it allows the antenna to be integrated with other fluidic components for tuning, sensing, and signal modulation, (iii) it does not involve etching or plating and thus does not produce hazardous waste. There are, however, challenges associated with shaping the fluid metal into more complex geometries that go beyond simple dipoles (such as the co-planar, sheet-like geometry of a patch or aperture to coupled slot antenna) due to non-uniform filling of wide microchannels. In addition, using metal liquid alone within a flexible host polymer has shown very often a poor mechanical durability.[14,15]

In this letter we report on the incorporation of single walled carbon nanotubes (SWNTs) within a EGaIn metal liquid alloy, yielding the fabrication of a fluidic flexible patch antenna operating at 4 GHz (S-band), thereby obtaining a radiating antenna-structure element with improved electrical properties and stable mechanical durability. Based on our simulations results, we used our developed UV-assisted direct-writing technology to design the patch antenna onto a PDMS substrate, followed by injecting and encapsulating the conductive EGaIn/SWNT nanocomposites—with varying SWNTs loads—that serve as a radiant antenna element material. The fluidic antennas specimen exhibited excellent performance in total agreement with our simulations. The room temperature *dc* electrical conductivities of these antenna devices were shown to increase with respect to SWNT concentration in the nanocomposite and were about 2 orders of magnitude higher than that of the pure EGaIn, when SWNT loads range from 0.5 to 5 wt. % only. More importantly, the associated reflection coefficient has increased up to |−10| dB

[a)]Author to whom correspondence should be addressed. Electronic addresses: aissab@emt.inrs.ca and brahim.aissa@mpbc.ca

for the same SWNT variation-range. Finally, the effect of the SWNTs on the long-term stability of the mechanical bending is also demonstrated over more than 12 months, which is a fundamental achievement towards realizing operating-stable bendable antenna devices based on SWNT and metal alloy nanocomposites.

Single wall carbon nanotubes were synthesized by using the developed plasma torch technology (detailed process can be found in Ref. 27). This process exclusively produces SWNTs that take growth in the gas-phase. The as-grown soot like SWNTs were subsequently purified by an acidic treatment through refluxing in a 3M-HNO_3 (Sigma Aldrich) solution.[28,29]

The SWNTs were characterized by bright field transmission electron microscopy (TEM) using a Jeol JEM-2100 F FEG-TEM (200 kV) microscope. Figure 1(a) shows a representative TEM micrograph of the purified SWNT deposit, where bundles of a few SWNTs are containing individual tube diameters of about 1.2 nm. These bundles have diameters in the 2–10 nm range and lengths of the order of few μm leading thereby to SWNT having an aspect ratio over three orders of magnitudes. Purified SWNTs were first ultrasonicated in dimethylformamide (1 mg/ml) solution for 5 h to dissolve bundles, followed by centrifugation at 12 000 rpm for 15 min to select well-dispersed, narrow bundles of the SWNTs. The centrifuged solution was then held at 50 °C for solvent evaporation. This purification process is known to graft COOH carboxylic acid groups on the nanotube, an inherent consequence to the chemical process, which favours their dispersion.[28,29] Appropriate weights of purified SWNT were then dispersed inside a room temperature liquid EGaIn (Sigma Aldrich) using a wand-type ultrasonic processor (CP750, Cole Parmer) for 30 min. Figure 1(b) depicts the simulated geometry and dimensions of the radiating microstrip patch antenna operating at 4 GHz S-band frequency (MATLAB® solution and CST Microwave Studio® 2011 softwares were used for parameters calculations). The simulated parameters are summarised in Table I.

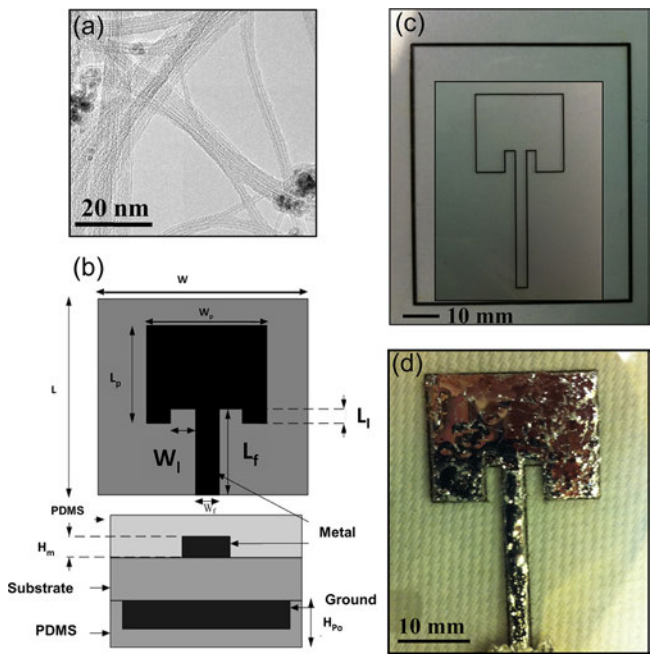

FIG. 1. (a) Representative TEM images of purified SWNTs. (b) Simulated geometry and dimensions of the radiating microstrip patch antenna operating at 4 GHz S-band frequency. (c) Optical top-view image of the epoxy/SWNT-based filaments deposited by UV-assisted direct writing technology on a PDMS substrate. (d) Optical top-view image of the infiltrated patch antenna element prototype.

UV-assisted direct writing technology[30–32] was then used to design the patch antenna onto a 500 μm-thick PDMS substrate. The fabrication of the radiant antenna structure began with the deposition of an epoxy/SWNT nanocomposite filament,[30,33] under continuous UV exposure[30] leading to a solid 2-D antenna pattern (Fig. 1(c)). The shape designed by the nanocomposite filaments was then filled with the EGaIn/SWNTs nanocomposite. The final specimen was then sealed to protect the liquid nanocomposite inside the sample; a 250 μm of PDMS was gently spin-coated to encapsulate the fluidic radiant element, followed by a curing step at 85 °C for 1 h. A V-type feed connector was appropriately incorporated to measure antenna performances. Figure 1(d) shows an optical top-view image of the infiltrated patch antenna prototype.

Figure 2(a) shows the relationship between the experimentally measured electrical conductivity (σ) of the elaborated EGaIn/SWNT nanocomposites with respect to their nanotube contents (using a Hewlett-Packard 4140B semiconductor parameter analyzer). With an increase of SWNT content, the conductivity gradually increases and is about 2 orders of magnitude higher than that of pure EGaIn, when SWNT loads reach ~5 wt. % only. The stepwise change in the conductivity of the composites is a direct result of the gradual formation of an interconnected network of SWNT inside the nanocomposite. Figure 2(b) shows the reflection coefficient S_{11}, as a function of the frequency, for both simulation and experiment scenarios (using an Agilent 8722ES network analyzer). The experimental results show that S_{11} increases from |−20| dB for a pure EGaIn alloy to reach its highest value of |−30| dB for a SWNT load of 5 wt. %, meaning that 99% and 99.9% of the input power is radiated from antenna, respectively. Since the pure PDMS polymer is transparent to EM radiation, the measured reflection coefficient is definitely due to the presence of the conductive material (EGaIn and SWNT). Table II summarizes the main performance parameters of the simulated and fabricated fluidic antennas as a function of the SWNTs concentration inside the nanocomposite. The average experimental uncertainty was found about ±5% over tens measured prototypes.

TABLE I. Simulated parameters of the radiating microstrip patch antenna operating at 4 GHz S-band frequency.

Parameters	Values	Parameters	Values
H_m (mm)	0.1	L_p (mm)	22.8
$H_{po} = h_{sub}$ (mm)	1	W_i (mm)	2.78
W (mm)	80	L_i (mm)	6.5
L (mm)	80	$\varepsilon_{po} = \varepsilon_{sub}$	2.5
W_f (mm)	2.78	σ_{EGaIn} (S/cm)	3.4×10^4
L_f (mm)	40	σ_{SWNT} (S/cm)	8.5×10^5
W_p (mm)	24		

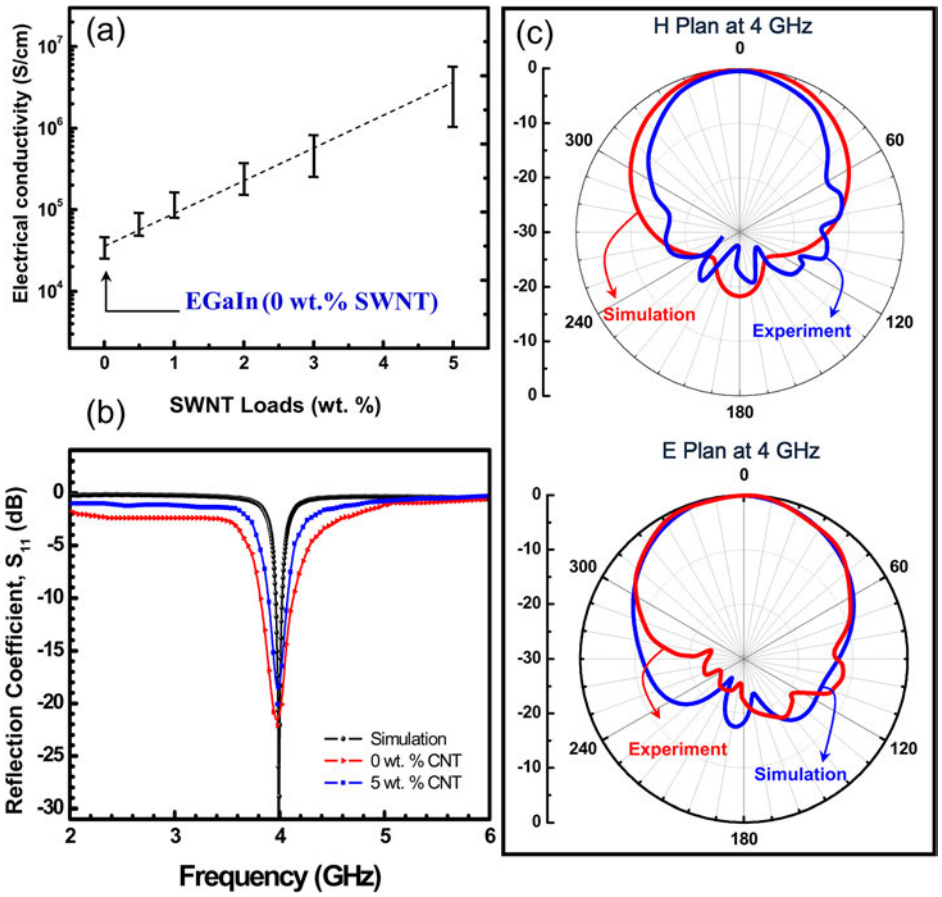

FIG. 2. (a) Relationship between the experimentally measured electrical conductivity σ_{dc} of the EGaIn/SWNT nanocomposite with respect to the nanotubes loads. (b) Reflection coefficient S_{11}, as a function of the frequency. (c) Corresponding simulated and experiment radiation patterns (H and E plans) at 4 GHz frequency.

The radiation patterns of the antenna prototype were measured inside an anechoic chamber with a Hybrid Near-Field Antenna Measurement System (HNFAMS) from Antcom Corp. Simulated and measured antenna radiation patterns in the E-plane and the H-plane are shown in Fig. 2(c). The fabricated antenna exhibits somehow an omnidirectional broad beam coverage. In fact, the radiation pattern, as expected, has a main lobe for the radiation of the patch in both the 0° pattern cut. Low gain in the direction of 180° below the ground plane confirms that the patch antenna does not radiate strongly in this direction. As seen in this figure, a good agreement between simulated and measured results was obtained. In addition, it can be noted that the fluidic prototype has the same performances in terms of bandwidth and radiation pattern compared to the conventional patch antenna.

The fabricated antenna prototypes were systematically bent inside a tube of particular curvature radius. Figure 3(a) shows the variation of the reflection coefficient as a function of the curvature radius for the simulated antenna and for the specimen fabricated with SWNT loads of 0 and 5 wt. %, respectively. When the bending angle of the antenna increases, the reflection coefficient decreases accordingly, and is even below the accepted value of |−10| dB for a curvature radius of 5 mm (recorded for the case of a pure EGaIn based prototype). At 30 mm curvature radius, all the antennas recover their initial radiation power (i.e., as that recorded before the bending). It is worth noting here that under the bending process, comparatively to the antenna specimen based on pure EGaIn (i.e., 0 wt. % of SWNT), the incorporation of 5 wt. % of nanotubes within the nanocomposite lead to a considerable improvement—up to 10 dB—of the associated reflection coefficients. This is ascribed to the enhancement of the global mechanical elasticity of the antennas brought by incorporating SWNT inside the nanocomposite. Figure 3(b) illustrates the change in the resonance frequency of the various antennas under different values of curvature. As expected, since the resonant frequency is rather related to the length of the radiant element and the effective dielectric constant of the medium,[7] no significant change is noticed, and the antenna specimens keep a stable radiation frequency within the experimental uncertainties.

Finally, we investigated the reliability of the antenna by repeatedly bent as a function of time. Table III summarizes the long-term performances of the antennas specimen (for two different SWNT loads, namely, 0 and 2 wt. %, respectively). Even after being bent over 100 times (12 months after the first measurement under ambient conditions), the antenna specimen containing 2 wt. % only of nanotube exhibited a return losses nearly the same (within 4.3%

TABLE II. Main antenna performance parameters (simulation and experiment) with respect to the nanotube contents into the nanocomposite.

CNT load (wt. %)	Simulations	0	0.5	1	2	3	5
Res. freq. (GHz)	4	4.03	4.02	4.01	4.01	4.02	4.02
$\lvert S_{11}\rvert$ (dB)	43	20	22	23	23	24	30
$\lvert FWHM\rvert_{GHz}$	0.2	2.16	2.08	2	1.7	1.5	1.2

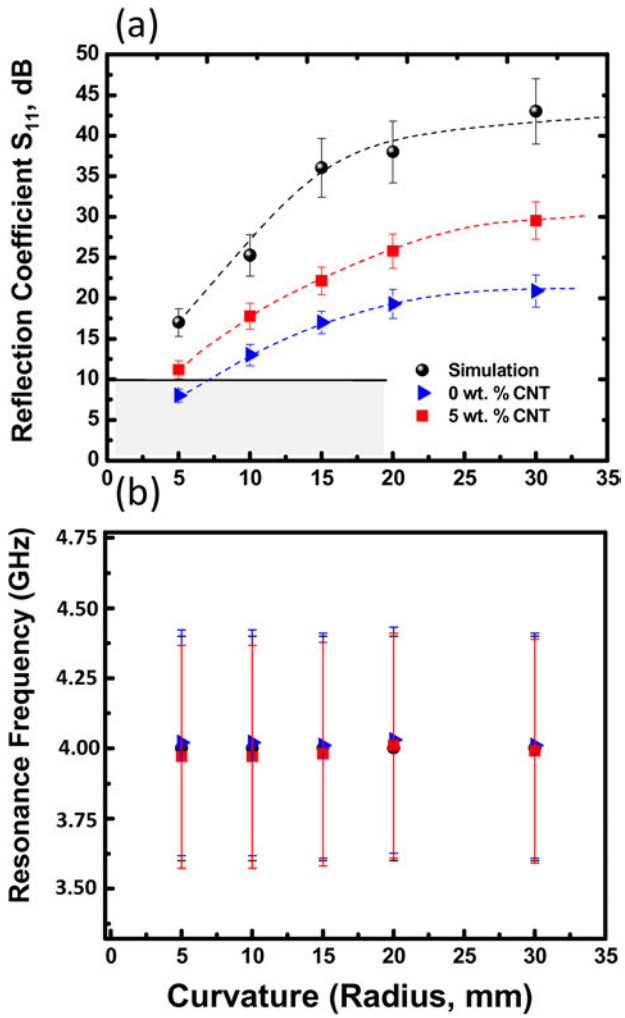

FIG. 3. (a) Return losses (reflection coefficient, S_{11}) at 4 GHz and (b) the resonance frequency for the simulated antenna, and these fabricated with SWNT loads of 0 and 5 wt. %, as a function of the curvature radius in mm.

fluctuation) as that of the initial measurement (the effect of the whole 0.5–5 wt. % loads of SWNTs on antenna performances is in progress). On the contrary, the specimen with no SWNT content manifests a fluctuation up to 13%. No changes were noticed for the resonance frequency parameter which remains stable in both cases (with and without SWNT). Thus, the combination of a liquid metal antenna with highly electrically conductive and mechanically elastic carbon nanotube materials resulted in an antenna structure that repeatedly returns to its original shape, even after multiple deformations, without losing its electromagnetic properties.

We note that the tendency revealed by Fig. 2(b) closely suggests a possible direct correlation between the S_{11} of the antenna specimens and their electrical conductivity (and hence with the SWNTs-concentrations within

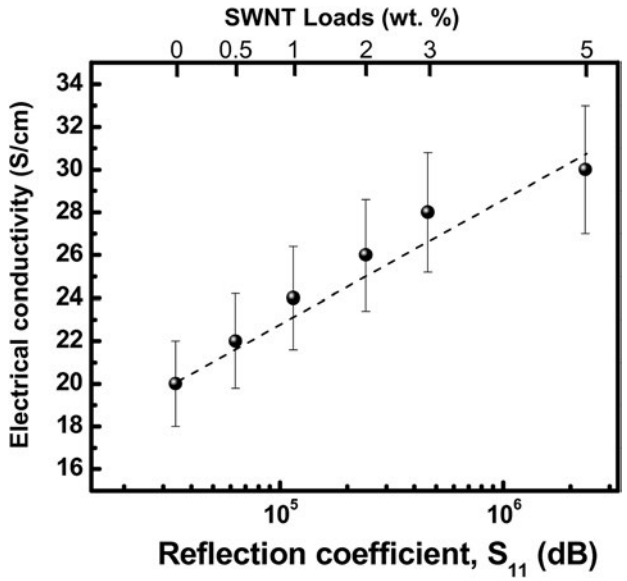

FIG. 4. Reflection coefficient (S_{11}) at 4 GHz for the whole fabricated prototypes as a function of their associated electrical conductivities σ_{dc} and SWNT loads.

the nanocomposite). By cross-plotting the S_{11} at 4 GHz of all the fabricated prototypes as a function of their associated σ_{dc} values, Figure 4 confirms that the antenna performances of all the investigated samples increase proportionally with respect to their electrical conductivity.[34] However, despite this experimental evidence, advanced characterizations and studies are required to determine the exact influence of the other involved factors, such as radiant-element thickness, and the effect of other frequency domains.

In summary, by using the UV assisted direct-writing technology, we demonstrated the fabrication of a fluid patch antenna based on a conductive nanocomposite material that consists of a liquid metal alloy (EGaIn) blended with SWNTs. The antennas prototypes, operating at the S-band frequency domain, have shown radiation characteristics of 90% efficiency and above (i.e., $>|-10|$ dB). These antennas have displayed a resonant frequency and return losses (S_{11}) capacity that are function of the SWNTs concentrations, in a good agreement with simulations modeling. The presented concept is promising for fluidic antennas that can be used in wireless sensing or monitoring radio systems, switches, RFID tags, conformal circuits for health monitoring, or in military and space applications.

We acknowledge financial support from the Canada Foundation for Innovation, the Natural Science and Engineering Research Council (NSERC) of Canada, the Fonds Québécois de la Recherche sur la Nature et les Technologies (FQRNT). F.R. is grateful to the Canada

TABLE III. Long-term antenna returns losses over storage under ambient conditions.

	Day 1	Month 1	Month 4	Month 7	Month 10	Month 12	Fluct.%
$\|S_{11}\|$ (dB) - 0 wt. % CNT	20	20	19	18.5	18	17	13%
$\|S_{11}\|$ (dB) - 2 wt. % CNT	23	23	23	23	22.5	22	4.3%

Research Chairs Program for partial salary support. B.A. is grateful to F. Larouche (Raymor Ind.) for supplying the SWNTs.

[1]S. H. Kim, C. Jang, K. J. Kim, S. Ahn, and K. C. Choi, IEEE Trans. Electron Devices **57**, 3370 (2010).
[2]J.-K. Lee, Y.-S. Lim, C.-H. Park, Y.-I. Park, C.-D. Kim, and Y.-K. Hwang, IEEE Electron Device Lett. **31**, 833 (2010).
[3]S. Merilampi, T. Björninen, L. Ukkonen, P. Ruuskanen, and L. Sydänheimo, Sens. Rev. **31**, 32 (2011).
[4]Y. K. Bekali and M. Essaaidi, Microwave Opt. Technol. Lett. **55**, 1622 (2013).
[5]J. H. Wang, L. Sang, Z. G. Wang, R. M. Xu, and B. Yan, J. Electromagn. Waves Appl. **27**, 330 (2013).
[6]E. Björnson, P. Zetterberg, M. Bengtsson, and B. Ottersten, IEEE Commun. Lett. **17**, 91 (2013).
[7]J. T. Bernhard, in *Reconfigurable Antennas, Encyclopedia of RF and Microwave Engineering*, edited by K. Chang (Wiley, New York, 2005).
[8]J.-C. Langer, C. Liu, and J. T. Bernhard, IEEE Microw. Wirel. Compon. Lett. **13**, 120 (2003).
[9]P. S. Hall and S. J. Vetterlein, IEE Proc. H **137**(5), 293 (1990).
[10]N. Tiercelin, P. Coquet, R. Sauleau, V. Senez, and H. Fujita, J. Micromech. Microeng. **16**, 2389 (2006).
[11]V. Lumelsky, M. Shur, and S. Wagner, IEEE Sens. J. **1**, 41 (2001).
[12]R. H. Reuss, B. R. Chalamala, A. Moussessian, M. G. Kane, A. Kumar, D. C. Zhang, J. A. Rogers, M. Hatalis, D. Temple, G. Moddel *et al.*, Proc. IEEE **93**, 1239 (2005).
[13]L. Gatzoulis and I. Iakovidis, IEEE Eng. Med. Biol. Mag. **26**, 51 (2007).
[14]J.-H. So, J. Thelen, A. Qusba, G. J. Hayes, G. Lazzi, and M. D. Dickey, Adv. Funct. Mater. **19**, 3632 (2009).
[15]S. Cheng, A. Rydberg, K. Hjort, and Z. Wu, Appl. Phys. Lett. **94**, 144103 (2009).
[16]R. C. Chiechi, E. A. Weiss, M. D. Dickey, and G. M. Whitesides, Angew. Chem., Int. Ed. **47**, 142 (2008).
[17]M. D. Dickey, R. C. Chiechi, R. J. Larsen, E. A. Weiss, D. A. Weitz, and G. M. Whitesides, Adv. Funct. Mater. **18**, 1097 (2008).
[18]T. Sekitani, Y. Noguchi, K. Hata, T. Fukushima, T. Aida, and T. Someya, Science **321**, 1468 (2008).
[19]C. Kim, Z. Wang, H.-J. Choi, Y.-G. Ha, A. Facchetti, and T. J. Marks, J. Am. Chem. Soc. **130**, 6867 (2008).
[20]A. C. Siegel, S. T. Phillips, M. D. Dickey, N. Lu, Z. Suo, and G. M. Whitesides, Adv. Funct. Mater. **20**, 28 (2010).
[21]L. Gatzoulis and I. Iakovidis, IEEE Eng. Med. Biol. Mag. **26**, 51 (2007).
[22]B. A. Cetiner, H. Jafarkhani, J.-Y. Qian, H. J. Yoo, A. Grau, and F. De Flaviis, IEEE Commun. Mag. **42**, 62 (2004).
[23]C.-P. Lin, C.-H. Chang, Y. T. Cheng, and C. F. Jou, IEEE Antennas Wireless Propag. Lett. **10**, 1108 (2011).
[24]H.-J. Kim, C. Son, and B. Ziaie, Appl. Phys. Lett. **92**, 011904 (2008).
[25]D.-H. Kim, J.-H. Ahn, W.-M. Choi, H.-S. Kim, T.-H. Kim, J. Song, Y. Y. Huang, L. Zhuangjian, L. Chun, and J. A. Rogers, Science **320**, 507 (2008).
[26]D.-H. Kim, J. Z. Song, W. M. Choi, H. S. Kim, R. H. Kim, Z. J. Liu, Y. Y. Huang, K. C. Hwang, Y. W. Zhang, and J. A. Rogers, Proc. Natl. Acad. Sci. U.S.A. **105**, 18675 (2008).
[27]O. Smiljanic, F. Larouche, X. L. Sun, J. P. Dodelet, and B. L. Stansfield, J. Nanosci. Nanotechnol. **4**, 1005 (2004).
[28]B. Aïssa, L. L. Laberge, M. A. Habib, T. A. Denidni, D. Therriault, and M. A. El Khakani, J. Appl. Phys. **109**, 084313 (2011).
[29]B. Aïssa, E. Hafeez, N. Tabet, M. Nedil, D. Therriault, and F. Rosei, Appl. Phys. Lett. **101**, 043121 (2012).
[30]L. L. Lebel, B. Aïssa, M. A. El Khakani, and D. Therriault, Adv. Mater. **22**, 592 (2010).
[31]B. Aïssa, E. Haddad, W. Jamroz, S. Hassani, R. D. Farahani, P. G. Merle, and D. Therriault, Smart Mater. Struct. **21**, 105028 (2012).
[32]D. Therriault, S. R. White, and J. A. Lewis, Nature Mater. **2**, 265 (2003).
[33]An Epon 828 based epoxy and SWNT nanocomposite filament of about 100 μm in thickness was first deposited onto the PDMS substrate and serve as structural walls to contain the metal fluidic alloy nanocomposite.
[34]C.-S. Zhang, Q.-Q. Ni, S.-Y. Fu, and K. Kurashiki, Compos. Sci. Technol. **67**, 2973 (2007).